FATIGUE BEHAVIOUR OF SILICON NITRIDE STUDIED BY INDENTATION FLEXURE METHOD

PAVOL HVIZDOŠ

Fatigue crack growth has been studied in self-reinforced gas pressure sintered silicon nitride (GPS Si_3N_4) using four-point bending of indented samples (indentation flexure fatigue – IFF) at room temperature under static and cyclic conditions. The method is simple, cost-effective, material and time saving, and produces stable crack growth. However, the analysis requires an estimation of the residual stress intensity factors produced by the indentations and assumptions about the shape of the indentation flaws to calculate the applied stress intensity factors. Crack growth parameters were calculated assuming a Paris's power law dependence. It was found that crack growth resistance was significantly reduced under cyclic loading due to the wear of the bridging ligaments in the crack wake. In the case of static fatigue, the resulting Paris's exponent was compared with the value obtained from the dynamic fatigue constant stress rate testing in 4-point bending using different loading rates. The crack growth mechanisms were identified using scanning electron microscope and have been correlated to the results of the fatigue tests.

ÚNAVA NITRIDU KREMÍKA ŠTUDOVANÁ METÓDOU OHYBU INDENTOVANÝCH VZORIEK

Únavové vlastnosti nitridu kremíka spekaného pod pretlakom dusíka (GPS Si_3N_4) sme študovali pomocou štvorbodového ohybu indentovaných vzoriek pri izbovej teplote v statickom a cyklickom režime. Táto jednoduchá a úsporná metóda umožňuje dosiahnuť stabilný rast trhliny, avšak analýza napäťového stavu v jej špici vyžaduje odhady tvaru indentačnej trhliny a veľkosti zvyškového faktora intenzity napätia, ktorý má pôvod vo vtláčaní. Vychádzajúc z Parisovho vzťahu, vypočítali sme parametre rastu trhliny. Pri cyklickom zaťažovaní bola odolnosť voči rastu trhliny značne nižšia kvôli opotrebeniu kontaktov premosťujúcich trhlinu. Parisov exponent získaný pri statickej únave sme porovnali s hodnotou získanou z dynamických skúšok v štvorbodovom ohybe pri rozličných rýchlostiach zaťažovania. Mechanizmy rastu trhliny sme identifikovali pomocou rastrovacieho elektrónového mikroskopu a posúdili sme ich vo vzťahu k výsledkom únavových skúšok.

K e y w o r d s: silicon nitride, indentation, fatigue, slow crack growth

RNDr. P. Hvizdoš, CSc., Ústav materiálového výskumu SAV, Watsonova 47, 043 53 Košice, SR. e-mail: hvizdos@saske.sk

1. Introduction

Evaluation of fatigue behaviour is essential to life-time prediction of materials as fatigue failure by the slow propagation of cracks under static or cyclic loads may be a critical problem for ceramics used for structural applications. There are several ways of characterizing the fatigue behaviour: static, cyclic and dynamic fatigue tests with or without artificial flaws, and direct v–K measurements by fracture mechanics test techniques [1], as well. In the past two decades there have been number of reports on the cyclic [1–4], static [1, 3, 5] and dynamic [1, 5] fatigue behaviour. Previous work on the fatigue of ceramics has been done on the alumina, zirconia and silicon nitride by applying the same techniques as used for metals, such as direct push-pull, compact tension (CT) or controlled surface crack (CSF). "Small" fatigue cracks (< 500 μm) are more typical of real applications, and cracks obtained by indentation are more similar to machining or natural flaws. As Tajima et al. [1] pointed out, there is no guarantee that the fatigue behaviour is identical for the naturally and artificially flawed specimens. For this reason, the indentation flexure fatigue (IFF) technique has been applied to study cyclic fatigue in structural ceramics [6–8]. The method produces stable crack growth therefore it is ideal for studying materials with large stress exponents and for studying materials at high temperatures.

The purpose of this study was to use the IFF method to characterize the room temperature static and cyclic fatigue crack growth behaviour of gas-pressure sintered silicon nitride, to compare the results with those obtained under dynamic loading conditions, and to investigate the advantages and disadvantages of the method.

2. Experimental

2.1 Material

Fatigue crack growth has been studied in self-reinforced silicon nitride – gas-pressure sintered Si_3N_4. The material was an experimental grade of the Si_3N_4 with 5 wt.% Yb_2O_3 as sintering additive made by Kyocera Corp., Japan. It was submitted in form of rectangular bending bars with dimensions of $3 \times 4 \times 45$ mm.

2.2 Experimental methods

2.2.1 *Indentation flexure fatigue (IFF)*

Fatigue tests were carried out using the indentation flexure method. The tensile surfaces of the specimens were ground and polished down to a 1 μm diamond paste finish. Series of Vickers indents of 98, 196 and 294 N loads were introduced within the inner spans on the tensile surfaces. The indents were spaced at least 1 mm apart in order to prevent interaction of the created radial indentation cracks

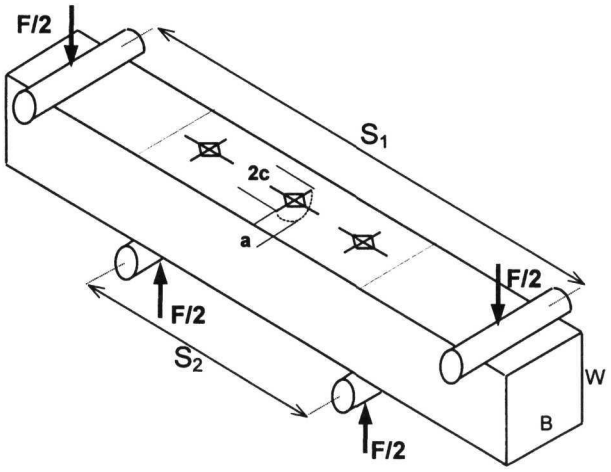

Fig. 1. Schematic drawing of the IFF test specimens with introduced indents.

and aligned so that these cracks were parallel or perpendicular to the long axis of the specimen. The geometry of the specimens and the indents are shown in Fig. 1. The prepared specimens were tested in four-point bending at room temperature in ambient air atmosphere. Inner/outer spans of 20/40 mm were used. Static and cyclic tests were carried out using a servohydraulic testing machine (Instron 8500).

Flexural stress, σ, experienced on the tensile surface between the inner rollers in four point bending was calculated from a standard formula

$$\sigma = \frac{3}{2} F \frac{S_1 - S_2}{BW^2}, \tag{1}$$

where F is the bending load.

The stress intensity factor induced by remote (outer surface) bending stress at the crack tip subjected to pure bending was calculated by Newman and Raju [9] as a function of the surface crack length, c, crack depth, a, and specimen height, W, using the finite element method. For semielliptical surface crack on the tensile surface of bending bar, they found

$$K_{\text{app}} = \frac{MS}{Q} B\sigma\sqrt{\pi a}, \tag{2}$$

where B is the bending multiplier, M, S, Q are geometric functions of a and W.

At room temperature the total stress intensity factor, K_{tot}, at the crack tip of the indentation crack subjected to bending was calculated as a sum of the residual

component, produced by the plastic zone beneath the indent impression, and the applied stress intensity factor

$$K_{\text{tot}} = K_{\text{res}} + K_{\text{app}} = \chi \frac{P}{c^{3/2}} + \frac{MS}{Q} B\sigma\sqrt{\pi a}. \tag{3}$$

K_{res} was evaluated according to Anstis et al. [10], where χ is a dimensionless indenter-material constant depending on the test geometry and physical properties of the tested material, P is the indentation load used, c is the indentation radial crack length at the surface. The crack depth, a, was estimated using the formula $a/W + a/c = 1$ according to the ASTM standard E740 [11].

In order to evaluate χ, it is necessary to know independently measured value of the fracture toughness, K_{IC}. This was obtained using the Single Edge V-Notch Beam method (SEVNB) for three flexure bars according to the procedure developed by the European Structural Integrity Society / Technical Committee 6 (ESIS/TC6), described in the Round-Robin instructions [12]. The V-notches were prepared to a radius of ~ 10 μm by polishing with a razor blade covered with 0.25 μm diamond paste. The notch geometry is documented in Fig. 2. The notched specimens were broken at a crosshead speed of 0.5 mm/min. The values of fracture toughness were calculated using the following formula [13]:

$$K_{\text{IC}} = \frac{F}{B\sqrt{W}} \frac{S_1 - S_2}{W} \frac{3\sqrt{\alpha}}{2(1-\alpha)^{1.5}} \gamma, \tag{4}$$

where geometric factor $\gamma = 1.9887 - 1.326\alpha - \dfrac{(3.49 - 0.68\alpha + 1.35\alpha^2)\alpha(1-\alpha)}{(1+\alpha)^2}$, and α is the normalized notch depth (a/W). Then, assuming $K_{\text{res}} = K_{\text{IC}} = \chi P/c^{3/2}$ at the crack tip after indentation, the constant χ can be found.

Fig. 3 schematically illustrates the applied, residual and total stress intensity factors as functions of crack length for an ideal test calculated according to Eq. (1). The profile of the K_{tot}-curve illustrates the main advantage of the indentation flexure method, the fact that it can produce stable crack growth. After indentation a radial crack will achieve an arrested/equilibrium length of c_1 and $K_{\text{tot}} = K_{\text{res}}$. This will not occur immediately because the final stage of crack growth is achieved by subcritical crack growth (SCG). By applying a

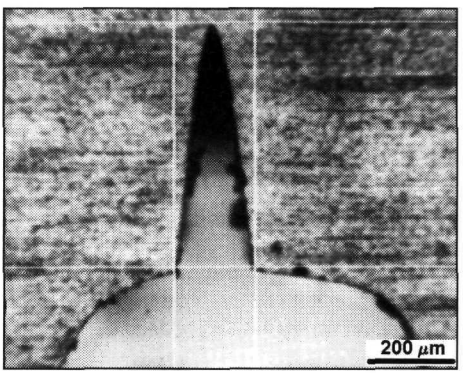

Fig. 2. Sharp notch prepared by polishing with a razor blade.

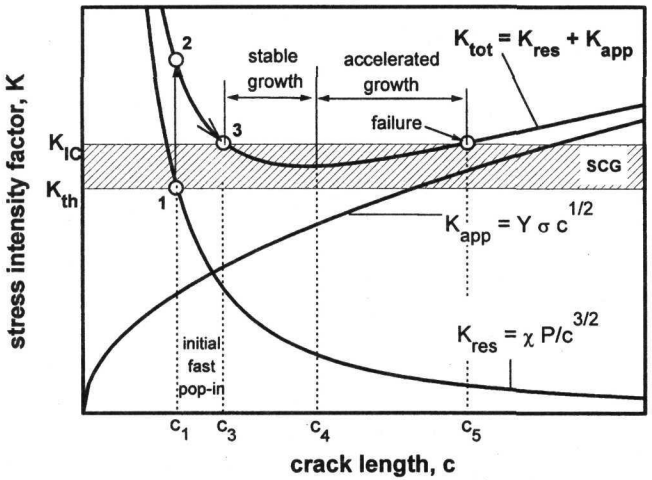

Fig. 3. Applied, residual, and total stress intensity factors at crack tip for an idealised indentation fatigue test as functions of the crack length.

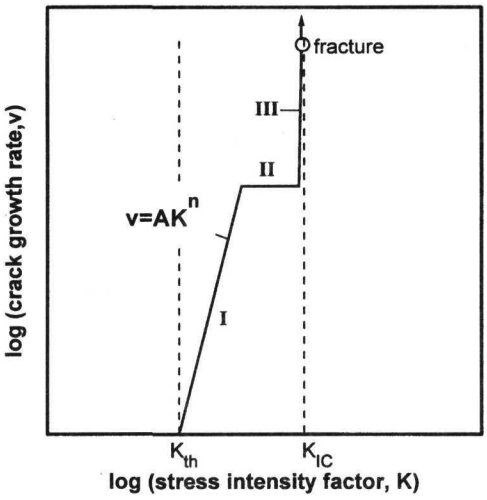

Fig. 4. Schematical illustration of the dependence of subcritical crack growth rate on stress intensity factor.

bending load a crack can be made to grow. The K_{tot} may exceed K_{IC} and the crack will propagate rapidly, "pops-in", to length c_3. The crack will then grow stably to length c_4, after which it will grow with increasing velocity to c_5 where it achieves a critical length resulting in fracture of the specimen.

Fig. 4 shows an idealised subcritical crack growth behaviour for a ceramic material [14, 15]. There may be some threshold value of stress intensity, K_{th}, below which a crack will not grow. It would be difficult to prove the existence of such a threshold because rapidly decreasing crack growth rates below a certain level are difficult to measure practically. In region II and III the crack growth rates are typically $\geq 1 \times 10^{-5}$ m/s, and once the cracks are growing at these sorts of rates, the specimens break very quickly. Therefore, it is usually the fatigue crack growth behaviour

in region I that is of most interest and is intensively studied. In order to describe the subcritical crack growth behaviour in region I the empirical power law relation, so-called Paris's law, between the stress intensity factor, K, and the crack growth rate, ν, is used

$$\nu = \frac{\mathrm{d}a}{\mathrm{d}t} = AK^n \quad \text{for} \quad K > K_{\mathrm{th}}, \tag{5}$$

where A and n are constants which can be calculated from $\log \nu - \log K$ plot.

After indentation, the crack lengths were measured at least one day later so that we could be sure that they had reached their equilibrium lengths. Then the specimens were subjected to their chosen test bending stress for 30 seconds. This allowed the cracks to pop-in. Depending on the testing conditions and the initial crack lengths, the crack typically grew by 0 to 30 μm during pop-in. Following pop-in, the new crack lengths were measured. The specimens were then reloaded and the actual fatigue test begun. This procedure meant that only crack growth associated with subcritical behaviour could be studied and that no overestimation of the crack velocity was made as a consequence of including the pop-in growth. The testing was stopped periodically (usually after $\sim$ 1 hour) to measure the crack growth.

The measurements of the crack lengths were made using an optical microscope. The corresponding K was estimated as the average of the K_{tot} for the initial and final crack lengths. The average crack propagation velocity was calculated by dividing the crack elongation by the test duration. If after series of measurements the specimen was not broken and the velocity of the crack propagation became too low (usually less than 10^{-10} m/s), a new higher bending stress was chosen and testing was continued again after the initial pop-in procedure. The cyclic tests were conducted with sinusoidal wave-forms at a test frequency, f, equal to 1 Hz, and load ratio $R = K_{\mathrm{min}}/K_{\mathrm{max}} = 0.1$. Values of K_{max} were used to plot the $\nu - K$ data for the cyclic tests. The crack growth rates under static loading, $\mathrm{d}a/\mathrm{d}t$, and cyclic loading, $\mathrm{d}a/\mathrm{d}N$, can be compared using

$$\frac{\mathrm{d}a}{\mathrm{d}t} = \frac{\mathrm{d}a}{\mathrm{d}N} f. \tag{6}$$

Following the mechanical tests, the fracture surfaces and fracture paths of the surface and subsurface fatigue cracks were studied using scanning electron microscope (JEOL JSM-6300) with the aim of identifying the fracture and fatigue damage mechanisms.

2.2.2 *Dynamic fatigue*

In order to verify the results by comparison with those measured by another method, the dynamic fatigue approach was used. In this case, combining the

Griffith's relation ($\sigma = YK_I/a^{1/2}$) with Paris's law of the fatigue crack growth (5), for values of bending strength (σ_{f1}, σ_{f2}) measured using two different constant stress rates ($\dot{\sigma}_1, \dot{\sigma}_2$), the following relation can be obtained:

$$\frac{\sigma_{f1}}{\sigma_{f2}} = \left(\frac{\dot{\sigma}_1}{\dot{\sigma}_2}\right)^{1/(n+1)} . \tag{7}$$

Thus, plotting the strength values as a function of stress rate on a log-log scale, the slope of the linear regression line is equal to $1/(n+1)$.

The dynamic fatigue tests were conducted in four-point bending mode with inner/outer spans 20/40 mm, in ambient air at room temperature. To introduce the defined flaws, the indentation impacts were made on the tensile surfaces using Vickers indenter under loading of 98 N. The indentations, one for each specimen, were placed to the centre between the inner rollers, and aligned the same way as in the case of the IFF tests. The specimens were tempered for 1 hour at 1200 °C prior to the tests in order to remove the residual stresses. Two specimens were used at each loading rate. The load-deflection curves were recorded up to specimen failure. Flexural strength (σ_f) was measured at four crosshead speeds, 0.01, 0.1, 1, and 10 mm/min, and calculated using Eq. (1).

3. Results and discussion

The microstructure of the GPS Si_3N_4 had a bimodal character and consisted of fine equiaxed grains with size of ~ 1 μm and uniformly distributed large whisker-like β-Si_3N_4 grains which were 20–30 μm long with the mean aspect ratio approximately equal to 5 (Fig. 5).

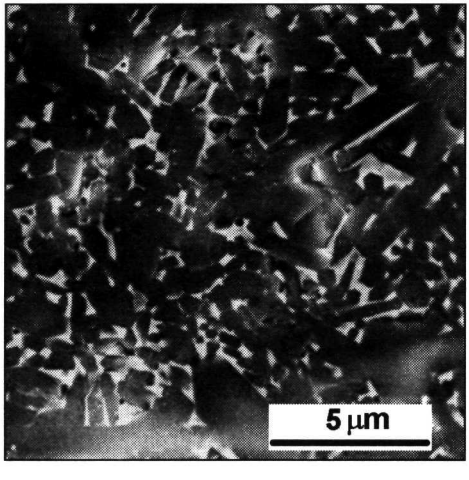

Fig. 5. Microstructure of the GPS Si_3N_4.

Mechanical properties of the experimental material at room temperature are shown in Table 1. The fracture toughness values measured by SEVNB method enabled us to calibrate the materials and geometry constant used in Eq. (3). A series of Vickers indentations, produced by 49, 98, 196, 294, and 490 N, were made on the polished surfaces of specimens. From the slope of $c^{3/2}$ vs. P plot in Fig. 6, the value of $\chi = 0.070$ was found. On the basis of this result the values of the residual stress intensity factors were calculated.

Table 1. Mechanical properties of the studied material

Material	Vickers hardness [GPa]	K_{IC}-SEVNB [MPa·m$^{1/2}$]	Bend strength [MPa]
Si_3N_4	15.5 ± 0.3	7.1 ± 0.5	850 ± 30

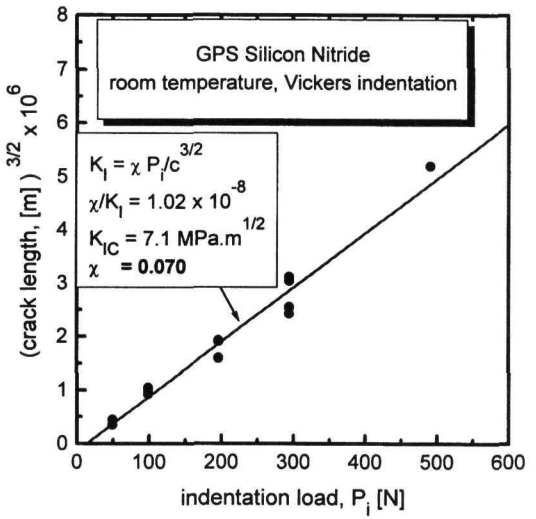

Fig. 6. Calibration of the indenter-material constant χ for calculating the residual stress intensity factor.

The results of IFF tests are shown in Fig. 7 where they are also compared to the results of Bermudo et al. [16] measured for materials with similar microstructure, hot pressed silicon nitrides, using the compact tension (CT) method. They obtained values of n between 27 and 31 for the cyclic data sets and 101–142 for the static data. Experimental material studied in this work exhibited very narrow region of possible subcritical crack growth under static load at room temperature. Thus, a very high stress exponent, 200, was found. Such a high value makes the measurement of the fatigue crack growth rates very difficult using other experimental methods. That is why only a few CT data points were presented by Bermudo et al. [16]. However, the stable character of the crack growth in IFF makes the experiments relatively easy to perform. On the other hand, the IFF method is very sensitive to the exact measurement of the crack dimensions and shape, which results in a relatively high scatter of data.

As it can be seen in Fig. 7, the IFF method tends to overestimate the stress

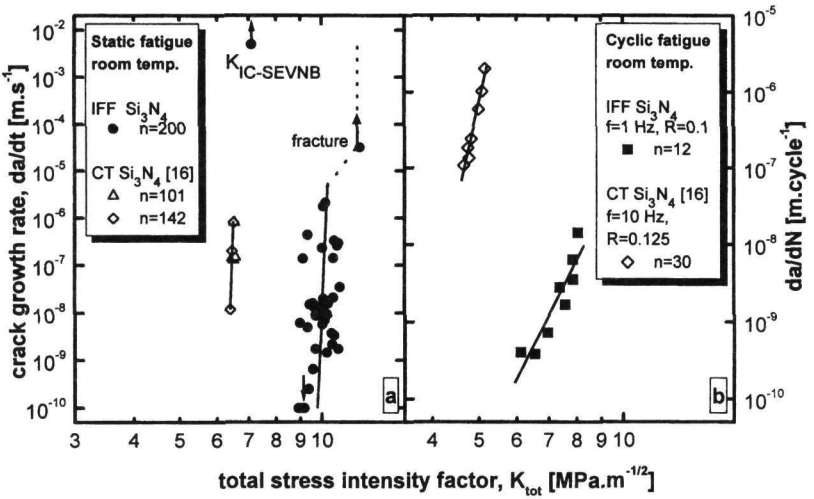

Fig. 7. Fatigue crack growth rates for the experimental materials at room temperature obtained using the IFF and compared with the CT data for similar materials: a) static mode, b) cyclic mode.

intensity factor values in comparison with K_{IC} measured by SEVNB. This is even more pronounced for materials that show a significant rising fracture toughness with crack length (R--curve behaviour), as it is the case for the GPS silicon nitride [17]. The crack lengths (typically 100–500 μm) in IFF are larger than the saturation crack lengths for R-curve behaviour (typically < 200 μm) [18] in these kinds of ceramics.

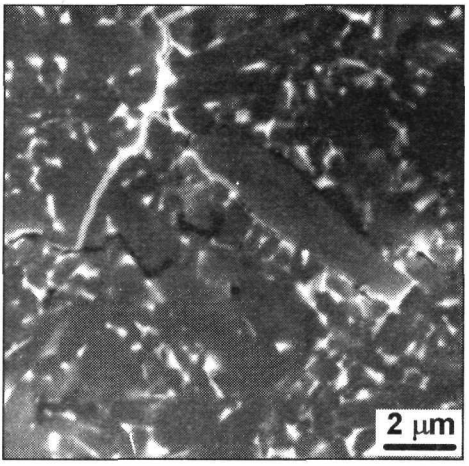

Fig. 8. SEM micrograph of fatigue crack in Si_3N_4 showing pull-out of β-Si_3N_4, crack deflection and crack bridging by grains at room temperature.

SEM studies of the crack growth mechanisms on the crack paths and crack surfaces showed frequent reinforcing by means of grain bridges and pulled-out elongated grains, as it is illustrated in Fig. 8. This corresponds well with relatively high K_{IC} of the material, and suggests R-curve behaviour. Predominantly intergranular fracture of

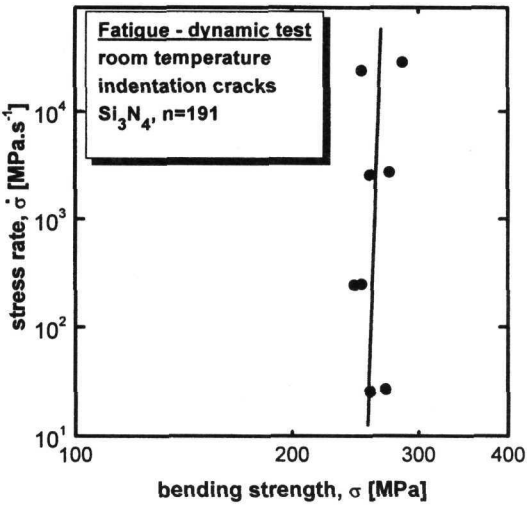

Fig. 9. Results of the dynamic fatigue test in a form of stress rate vs. strength plot. The slope is equal to $n + 1$.

this type of Si_3N_4 points toward oxide grain boundary phases as the cause of the delayed failure-slow crack growth, as also suggested by other investigators [3, 19]. Absence of the oxide additions, e.g. in CVD Si_3N_4 or RSSN, was reported to lead to exclusively or predominantly transgranular fracture and to prohibit any delayed failure [20].

Fig. 9 shows the results of the dynamic fatigue tests done at different stress rates. The load-displacement curves showed pure elastic behaviour up to the failure. The value of $n = 191$ is in a very good agreement with the static fatigue tests results. This fact confirms the feasibility of the IFF method. We note that in order to obtain this single result by the dynamic method, eight specimens, all flawed by the same type (shape and size) of cracks, were used, each giving just one point to the stress rate – stress plot. At the same time, only one specimen, covering a range of lengths of the indentation cracks, was used in the IFF method.

Fig. 7b shows results obtained under cyclic conditions. The material exhibited considerably lower fatigue resistance (lower K_s) than under static conditions and also much smaller stress exponents compared to static conditions ($n = 12$ for the cyclic fatigue in comparison to $n = 200$ for the static conditions). The cyclic fatigue behaviour of silicon nitride has been actively investigated [21, 22] because mechanical degradation under cyclic load conditions is relevant to the engineering application of silicon nitride. The fatigue in Si_3N_4 has been attributed to microstructural damage produced by the cyclic nature of stress. This behaviour

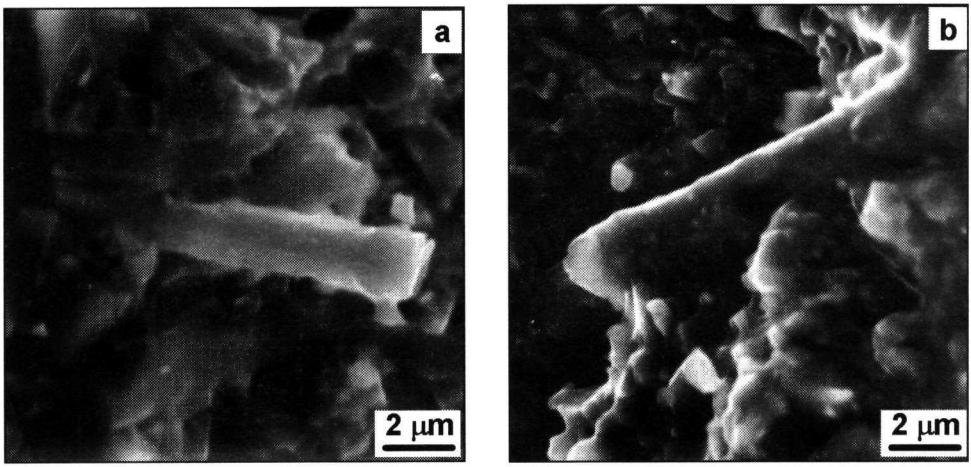

Fig. 10. Fracture surfaces from the subcritical crack growth area of the Si_3N_4 tested under (a) static and (b) cyclic loading, showing character of the crack surface asperities.

has been reported many times before [23–26] and numerous mechanisms have been proposed. In the used GPS Si_3N_4 with frequent toughening processes, such as crack deflection and bridging, whisker pull-out, interfacial friction, the mechanical degradation is mostly caused by the sequential loss of interacting forces between the crack faces, and by the asperity contact. This asperity contact can result in the formation of lateral cracks at crack surface asperities and in wedging effect during unloading [24]. The character of the fracture surfaces can be seen in Fig. 10, where the difference between statically (a) and cyclically (b) loaded samples is visible. In the case of the latter one, the reinforcing asperities wore off (Fig. 10b).

Comparison with the CT data [16] shows that for silicon nitride ceramics the IFF method gives results consistent with other methods, with respect to the n-values, being more time- and material-saving, and also considerably easier to perform.

4. Conclusions

The indentation flexure method provides a simple, inexpensive and highly cost-effective method for studying fatigue crack growth in ceramics. The method produces stable crack growth and it is particularly useful for studying crack growth in materials with large stress exponents.

For materials that show a significant rising fracture toughness with crack length (R-curve behaviour), the IFF data is significantly shifted toward higher K_s compared to K_{IC} (SEVNB). This is caused by the fact, that the crack lengths

(typically 100–500 μm) in IFF are larger than the saturation crack lengths for R-curve behaviour (typically < 200 μm). Comparison of the IFF results with the dynamic fatigue tests showed very good agreement in the obtained values of the stress exponent n. The uncertainty in the analysis of the data and the scatter of the data for the IFF method limits its usefulness. However, considering its practical advantages over other methods, it provides an excellent method for investigating the relative effect of loading conditions on fatigue crack growth. It also provides a good method for comparing the fatigue behaviour of different materials.

Comparing the static and cyclic fatigue behaviour showed, that strong contact toughening in the GPS Si_3N_4 results in great degradation under cyclic loading.

Acknowledgements

Part of the work was carried out during P. Hvizdoš's stay at Queen Mary and Westfield College in London supported by a NATO fellowship and by the Slovak Grant Agency under the contract no. 2/5162/98.

REFERENCES

[1] TAJIMA, Y.—URASHIMA, K.—WATANABE, M.—MATSUO, Y.: Static, cyclic and dynamic fatigue behavior of silicon nitride. In: Ceramic Materials & Composites for Engines. Ed.: Tennery, V. J. Las Vegas, American Ceramic Society 1988, p. 719.
[2] FETT, T.—HIMSOLT, G.—MUNZ, D.: Advanced Ceram. Mat., *1*, 1986, p. 179.
[3] KAWAKUBO, K.—KOMEYA, K.: J. Am. Ceram. Soc., *70*, 1987, p. 400.
[4] KOSSOWSKY, R.: J. Am. Ceram. Soc., *56*, 1973, p. 531.
[5] CHANG, J.—KHANDELWALL, P.—HEITMAN, P. W.: Ceram. Eng. Sci. Proc., *8*, 1987, p. 766.
[6] PETROVIC, J. J.—JACOBSON, L. A.—TALTY, P. K.—VASUDEVAN, A. K.: J. Am. Ceram. Soc., *58*, 1975, p. 113.
[7] LIU, S. Y.—CHEN, I.-Y.—TIEN, T. Y.: J. Am. Ceram. Soc., *77*, 1994, p. 137.
[8] ZHAN, G.-D.—REECE, M. J.—LI, M.—CALDERON-MORENO, J. M.: J. Mater. Sci., *33*, 1998, p. 3867.
[9] NEWMAN Jr., J. C.—RAJU, I. S.: Analysis of surface cracks in finite plates under tension or bending loads. NASA Technical paper 1578, 1979.
[10] ANSTIS, G. R.—CHANTIKUL, P.—LAWN, B. R.—MARSHALL, D. B.: J. Am. Ceram. Soc., *64*, 1981, p. 533.
[11] Standard recommended practice for fracture testing with surface-crack tension specimens. ASTM Standard E 740-80, ASTM Annual Book of Standards, Vol. 301, Philadelphia 1983, pp. 740–750.
[12] KÜBLER, J.: VAMAS TWP#3 / ESIS TC6 round robin on fracture toughness of ceramics using the SEVNB method. EMPA Dübendorf 1997.
[13] SRAWLEY, J. E.—GROSS, B.: In: Cracks in Fracture. Am. Soc. Test. Mater., Spec. Tech. Publ., No. 601, ASTM, Philadelphia 1976, p. 559.
[14] WIEDERHORN, S. M.—FREIMAN, S. W.—FULLER, E. R.—SIMMONS, C. J.: J. Mater. Sci., *17*, 1982, p. 3460.
[15] WIEDERHORN, S. M.: J. Am. Ceram. Soc., *50*, 1967, p. 407.
[16] BERMUDO, J.—OSENDI, M. I.—LI, M.—REECE, M. J.: J. Europ. Ceram. Soc., *17*, 1997, p. 1855.

[17] HVIZDOŠ, P.—JIANG, D.-Y.—REECE, M. J.: Key Eng. Mat., *175–176*, 1999, p. 253.
[18] DUSZA, J.—ŠAJGALÍK, P.—LOFAJ, F.: Key Eng. Mat., *89–9*, 1994, p. 517.
[19] GULDEN, M. E.—METCALFE, A. G.: J. Am. Ceram. Soc., *59*, 1976, p. 391.
[20] McKINNEY, K. R.—BENDER, B. A.—RICE, R. W.—WU, C. M.: J. Mat. Sci., *26*, 1991, p. 6467.
[21] OKAZAKI, M.—McEVILY, A. J.—TANAKA, T.: Met. Trans. A, *22*, 1991, p. 1425.
[22] OKAZAKI, M.—McEVILY, A. J.—TANAKA, T.: Mat. Sci. Eng. A, *143*, 1991, p. 135.
[23] GRATWOHL, G.: Mat.-wiss. u. Werkstoffentech., *19*, 1988, p. 113.
[24] EVANS, A. G.: Int. J. Frac., *16*, 1980, p. 485.
[25] REECE, M. J.—GUIU, F.—SAMMUR, M. F. R.: J. Am. Ceram. Soc., *72*, 1989, p. 348.
[26] KISHIMOTO, H.: JSME Int. J. Series I, *34*, 1991, p. 393.

Received: 3.3.2000